

Rate Equation Analysis of Frequency Chirp in Optically Injection-Locked Quantum Cascade Lasers

C. Wang,^{a,b*} F. Grillot,^a V. I. Kovanis,^{c,d} J. D. Bodyfelt,^e and J. Even^b

^aTelecom Paristech, Ecole Nationale Supérieure des Télécommunications, CNRS LTCI, 46 rue Barrault, 75013 Paris, France

^bUniversité Européenne de Bretagne, INSA, CNRS FOTON, 20 avenue des Buttes de Coësmes, 35708 Rennes Cedex 7, France

^cElectro Science Laboratory, The Ohio State University, 1320 Kinnear Road, Columbus, Ohio 43212, USA

^dAir Force Research Laboratory, 2241 Avionics Circle, Wright-Patterson AFB, Dayton, Ohio 45433, USA

^eMassey University Albany, Private Bag 102904, North Shore City, Auckland 0745, New Zealand

*cheng.wang@insa-rennes.fr

ABSTRACT

The frequency chirp characteristics of an optically injection-locked quantum cascade laser are theoretically investigated. The key parameter chirp-to-power ratio (CPR) is analytically derived from a full rate equation model. The CPR value can be efficiently reduced by increasing optical injection strength, especially at modulation frequencies less than 10 GHz. In contrast to interband lasers, both positive and negative frequency detuning increase the CPR. Since the frequency detuning is also predicted to enhance the intensity modulation response, a trade-off is required in the optical injection to simultaneously obtain a large modulation bandwidth and low frequency chirp.

Keywords: quantum cascade laser, injection locking, frequency chirp

1. INTRODUCTION

Conventional interband semiconductor lasers relying on the recombination of electrons and holes can hardly reach a lasing wavelength longer than 3 μm , due to the bandgap limitation in semiconductor heterostructures [1]. Nevertheless, thanks to the sophisticated electronic subband engineering, quantum cascade (QC) lasers offer an alternative solution to cover a wide wavelength interval ranging from mid-infrared up to terahertz frequencies [2]. Thus, QC lasers have extensive applications in gas sensing, telecommunication, spectroscopy and imaging [3], [4]. A unique feature of QC lasers is the ultrafast carrier relaxation time (on the order of several picoseconds), which is dominated by the longitudinal optical (LO)-phonon assisted scattering process [2]. This property makes QC lasers quite suitable for high-speed operation. For instance, generation of ultrafast pulses has been demonstrated by the gain switching and mode locking techniques [5], [6]. Furthermore, QC lasers show broadband modulation responses with a 3-dB bandwidth of tens of gigahertz, an order of magnitude larger than in the case of interband semiconductor lasers. In addition, because of the ultrafast intersubband transitions, a particular feature of QC lasers is the absence of relaxation oscillations, which are usually observed in conventional semiconductor lasers.

In order to boost the dynamical characteristics of semiconductor lasers, optical injection has been employed as an attractive technique over the past decades [7]. In that case, the injected laser property is driven by two key parameters: the injection ratio and the detuning frequency. The injection ratio is defined as the power ratio of the injected signal to the free-running laser signal, and the detuning frequency is the frequency shift of the injected signal with respect to the free-running frequency of the slave laser. Inside the stable-locked regime, injection locking is beneficial for enhancing the modulation bandwidth [7], reducing the frequency chirp [8], suppressing the relative intensity noise (RIN) [9] and the nonlinear distortion [10]. Outside the stable-locked regime, there are various periodic oscillations and even chaos, which are valuable for microwave generation and chaos applications [11]-[13]. Although the injection locking technique is

robust, its application to QC lasers remains little explored. Recent theoretical study of the optical injection-locked QC lasers has shown that both instability and bi-stability appears in the local bifurcation diagram [14]. A small-signal modulation of semiconductor laser device generates both amplitude and frequency modulations in the output optical signal. In our previous work, the intensity modulation behaviour of an injection-locked QC laser was analyzed [14], [15]. It was shown that a resonance appears in the positive detuning side of the stable-locked regime. This work aims to go a step beyond by investigating the frequency chirp behaviour of optical injection-locked QC lasers. It is found that the chirp-to-power ratio (CPR) is reduced by optical injection, and zero frequency detuning gives the minimum CPR value in comparison with other detuning frequencies. As for interband semiconductor lasers, the linewidth enhancement factor (LEF) plays an important role in the frequency chirp properties of QC lasers.

2. RATE EQUATION MODEL DESCRIPTION

QC laser device usually consists of tens of repeated cascading stages. In this work, it is assumed that all stages are uniform. Each stage contains one injector region and one active region. In the active region, three electronic states are taken into account. Figure 1 shows the schematic structure of the carrier dynamics in one stage. Electrons in the injector region are firstly injected into the upper laser state of the active region through a tunneling process. Then the electrons either relax to the lower laser state by radiative emission within time τ_{32} or to the bottom state within time τ_{31} . The lower laser state is depopulated through the ultrafast non-radiative resonant phonon scattering process within time τ_{21} . Finally, the carriers tunnel into the next stage (within τ_{out}).

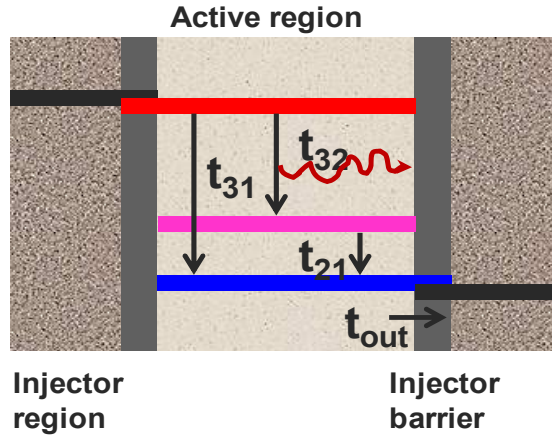


Figure 1. Sketch of carrier dynamics in one stage of a quantum cascade laser

Coupling the carrier dynamics and the complex electric field of an optical injection-locked laser, the rate equations for the injected QC laser are described by [16], [17]:

$$\frac{dN_3}{dt} = \eta \frac{I}{q} - \frac{N_3}{\tau_{32}} - \frac{N_3}{\tau_{31}} - G_0 \Delta N S \quad (1)$$

$$\frac{dN_2}{dt} = \frac{N_3}{\tau_{32}} - \frac{N_2}{\tau_{21}} + G_0 \Delta N S \quad (2)$$

$$\frac{dN_1}{dt} = \frac{N_3}{\tau_{31}} + \frac{N_2}{\tau_{21}} - \frac{N_1}{\tau_{out}} \quad (3)$$

$$\frac{dS}{dt} = (N_{pd} G_0 \Delta N - 1 / \tau_p) S + \beta N_{pd} \frac{N_3}{\tau_{sp}} + 2k_c \sqrt{S_{inj}} S \cos \phi \quad (4)$$

$$\frac{d\phi}{dt} = \frac{\alpha_H}{2} (N_{pd} G_0 \Delta N - 1 / \tau_p) - \Delta \omega_{inj} - k_c \sqrt{\frac{S_{inj}}{S}} \sin \phi \quad (5)$$

where $N_{3,2,1}$ are the carrier numbers in each state, and S is the photon number. The phase difference between the slave laser and the master laser is $\phi = \phi_{slave} - \phi_{master}$. $G_0 = G_d (1 - \xi S)$ with the linear gain coefficient G_d and the gain

compression factor ξ . The population inversion is $\Delta N = N_3 - N_2$, and N_{pd} denotes the stage number. τ_p is the photon lifetime, τ_{sp} is the spontaneous emission time and β is the spontaneous emission factor. k_c is the coupling rate of the master laser into the slave laser which is $k_c = c(1-R)/(2n_r L \sqrt{R})$ with n_r the refractive index and L is the cavity length. The detuning frequency is defined by $\Delta\omega_{inj} = \omega_{master} - \omega_{slave}$, and the injection ratio is $R_{inj} = S_{inj}/S_{FE}$ with the injected photon number S_{inj} and the free-running photon number S_{FE} .

In the small-signal analysis of the rate equations, a small-signal ac current $i_1 \exp(j\omega t)$ is superimposed to the dc bias current I . Consequently, the carrier number, photon number and phase will also vary around their dc values: $N_x(t) = N + n_x \exp(j\omega t)$, $S(t) = S + s_1 \exp(j\omega t)$, and $\phi(t) = \phi + \phi_1 \exp(j\omega t)$. Then, the linearized rate equation in the matrix form is:

$$\begin{bmatrix} \gamma_{11} + j\omega & -\gamma_{12} & 0 & -\gamma_{14} & 0 \\ -\gamma_{21} & \gamma_{22} + j\omega & 0 & -\gamma_{24} & 0 \\ -\gamma_{31} & -\gamma_{32} & \gamma_{33} + j\omega & 0 & 0 \\ -\gamma_{41} & -\gamma_{42} & 0 & \gamma_{44} + j\omega & -\gamma_{45} \\ -\gamma_{51} & -\gamma_{52} & 0 & -\gamma_{54} & \gamma_{55} + j\omega \end{bmatrix} \begin{bmatrix} n_3 \\ n_2 \\ n_1 \\ s_1 \\ \phi_1 \end{bmatrix} = \frac{\eta i_1}{q} \begin{bmatrix} 1 \\ 0 \\ 0 \\ 0 \\ 0 \end{bmatrix} \quad (6)$$

with

$$\begin{aligned} \gamma_{11} &= G_0 S + \frac{1}{\tau_{32}} + \frac{1}{\tau_{31}}; & \gamma_{12} &= G_0 S; & \gamma_{14} &= -G_0 \Delta N + G_d \Delta N \xi S; \\ \gamma_{21} &= G_0 S + \frac{1}{\tau_{32}}; & \gamma_{22} &= G_0 S + \frac{1}{\tau_{21}}; & \gamma_{24} &= G_0 \Delta N - G_d \Delta N \xi S; \\ \gamma_{31} &= \frac{1}{\tau_{31}}; & \gamma_{32} &= \frac{1}{\tau_{21}}; & \gamma_{33} &= \frac{1}{\tau_{out}}; & \gamma_{41} &= N_{pd} G_0 S + N_{pd} \frac{\beta}{\tau_{sp}}; \\ \gamma_{42} &= -N_{pd} G_0 S; & \gamma_{44} &= \frac{1}{\tau_p} - N_{pd} G_0 \Delta N - k_c \cos \phi \sqrt{\frac{S_{inj}}{S}} + N_{pd} G_d \Delta N \xi S; \\ \gamma_{45} &= -2k_c \sin \phi \sqrt{S_{inj} S}; & \gamma_{51} &= \frac{\alpha_H}{2} N_{pd} G_0; & \gamma_{52} &= -\frac{\alpha_H}{2} N_{pd} G_0; \\ \gamma_{54} &= \frac{k_c \sin \phi}{2S} \sqrt{\frac{S_{inj}}{S}} - \xi \frac{\alpha_H}{2} N_{pd} G_d \Delta N; & \gamma_{55} &= k_c \cos \phi \sqrt{\frac{S_{inj}}{S}} \end{aligned} \quad (7)$$

To analyze the intensity modulation response, the modulation transfer function is given by

$$H(\omega) = \left| \frac{s_1(\omega)}{\eta i_1 / q} \right| \quad (8)$$

The frequency chirp properties of semiconductor lasers can be characterized by the CPR, which value gives the frequency change for a given power deviation under modulation:

$$CPR = \left| \frac{j\omega \frac{\phi_1(\omega)}{s_1(\omega)}}{1} \right| = \frac{\alpha_H}{2S} \left| \frac{j\omega (j\omega + A + C)}{j\omega + B} \right| \quad (9)$$

with

$$\begin{aligned} A &= k_c \sqrt{\frac{S_{inj}}{S}} (\sin \phi / \alpha_H + \cos \phi); \\ B &= k_c \sqrt{\frac{S_{inj}}{S}} (\cos \phi - \alpha_H \sin \phi); \\ C &\approx \frac{\beta}{\tau_{sp}} \frac{\tau_{32} \tau_{21}}{\tau_{32} - \tau_{21}} N_{pd} \Delta N \left[G_0 (1 - \xi S) + \frac{\xi}{1 - \xi S} \frac{1}{\tau_{21}} \right]; \end{aligned} \quad (10)$$

Calculations show that the extracted CPR formula (equation (9)) for QC lasers is quite similar to that of interband lasers, except the expression of parameter C, which contains relaxation times τ_{32} , τ_{21} for the former case [18]. For the free-running QC laser without light injection, making A=0 and B=0, equation (9) reduces to

$$CPR_{FR} = \frac{\alpha_H}{2S} |j\omega + C| \quad (11)$$

Table 1. The QCL material and laser parameters used in the simulation.

Parameter	Value	Parameter	Value
Laser frequency ν	2.9 THz	Relaxation time τ_{32}	2.0 ps
Cavity length L	0.3 cm	Relaxation time τ_{31}	2.4 ps
Cavity width w	8×10^{-3} μm	Relaxation time τ_{21}	0.5 ps
Facet reflectivity R	0.29	Tunnelling out time τ_{out}	0.5 ps
Refractive index n_g	3.3	Photon lifetime τ_p	3.7 ps
Internal loss α_i	24 cm^{-1}	Spontaneous lifetime τ_{sp}	7.0 ns
Number of stage	30	Spontaneous emission factor β	1.0×10^{-6}
Gain coefficient G_d	$5.3 \times 10^4 \text{ s}^{-1}$	Linewidth enhancement factor α_H	0.5
Gain compression factor ξ	$5.0 \times 10^{-17} \text{ cm}^3$	Injection coupling rate k_c	20 GHz

3. RESULTS AND DISCUSSIONS

All the material and laser parameters used in the simulations are listed in table 1 [19], [20]. We firstly study the steady-state behaviour of the free-running laser without optical injection. As shown in Figure 2, the carrier number in the bottom state (dot line) increases linearly with the pump current, which follows the relation $N_1 = \tau_{out} \eta I / q$. Once above the lasing threshold (223 mA), the population inversion is almost clamped at a value of $\Delta N \approx 1 / (N_{pd} G_0 \tau_p)$. For the same device under optical injection, the laser threshold is traditionally reduced and the photon number is increased. In the following studies the bias current is set at $I_{bias} = 1.5 I_{th}$.

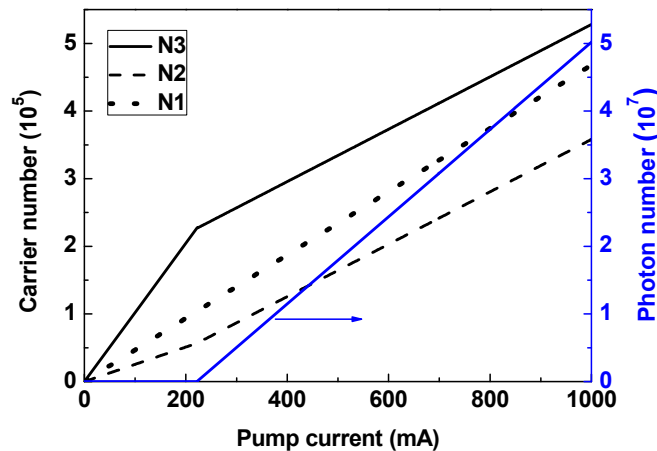


Figure 2. Steady-state properties of the studied free-running laser.

Before investigating the modulation properties, it is important to ensure that the laser is operated in the stable locking regime, which is bounded by the local bifurcations (saddle-node and Hopf) [21]. These bifurcations can be studied by the eigenvalue analysis and continuation computation method [22]. In the complex space, if a single, real eigenvalue passes through the imaginary axis, one finds a saddle-node bifurcation while a pair of complex conjugate eigenvalues crossing the imaginary axis corresponds to a Hopf bifurcation. The local bifurcation diagram in Figure 3 is calculated using the

continuation package Matcont [22]. High injection ratio enlarges the stable locking region, and a detuning range of about 30 GHz is obtained for an injection ratio of 10. The asymmetry of the locking diagram is due to the nonzero linewidth enhancement factor (LEF=0.5) of the laser [23]. The intensity modulation response of the laser can be calculated from equation (8). Figure 4(a) shows that the optical injection indeed enhances the modulation bandwidth in comparison with the free-running laser (solid line). In addition, both positive and negative frequency detunings lead to a peak in the modulation response. From the analysis of the eigenvalues, it is found that a resonance is induced for the positive frequency detuning case, which originates from the interaction between the locked field and the shifted cavity-resonance field [14], [24]. Figure 4(b) presents the 3-dB modulation bandwidth as a function of the detuning frequency. Each frequency detuning enhances the modulation bandwidth. Particularly, the positive detuning increases the bandwidth by more than 30 GHz.

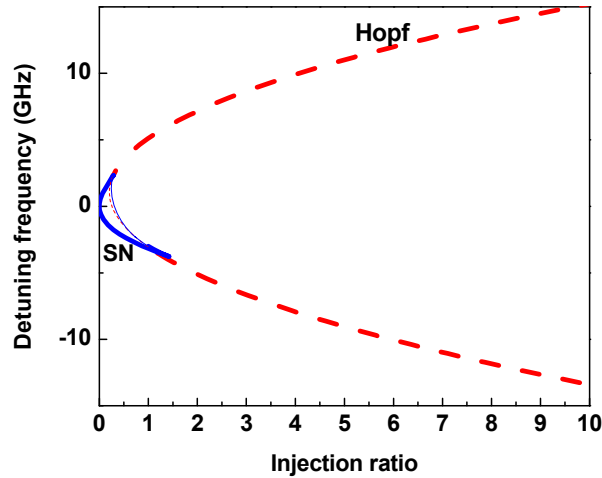


Figure 3. Local bifurcation diagram of the injection-locked QC laser with a linewidth enhancement factor of 0.5. The stable locked regime is bounded by both the saddle-node bifurcation (solid line) and Hopf bifurcation (dashed line).

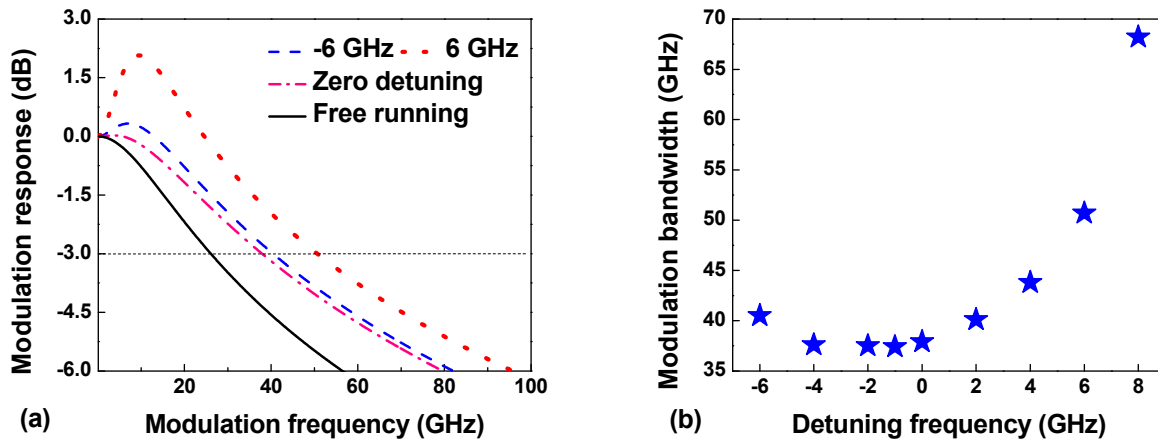


Figure 4. Frequency detuning effect of the injection-locked QC laser with an injection ratio of 5.0. (a) Intensity modulation response; (b) The 3-dB modulation bandwidth versus the detuning frequency.

Figure 5 shows the calculated CPR for the QC laser with and without optical injection. For the free running laser, the CPR remains almost constant in the modulation range 0.01~0.1 GHz. In this region, the adiabatic chirp dominates the chirp level originating from the gain compression as well as from the spontaneous emission according to equations (10) and (11). For higher frequencies than 0.1 GHz, the CPR increases almost linearly with the modulation frequency, and the slope is then determined by the linewidth enhancement factor and the laser output power. For the laser operating under optical injection, the constant CPR region vanishes because of the existence of the nonzero pole B in equation (9), which

value is determined by the injection ratio, phase difference and the linewidth enhancement factor. At zero detuning, the optical injection remarkably reduces the CPR level, especially for modulation frequencies less than 10 GHz. At the frequency of 1.0 GHz, the optical injection substantially decreases the free-running CPR from 480 MHz/mW down to 30 MHz/mW with an injection ratio of 10. For frequencies higher than 10 GHz, the modulation frequency dominates the CPR value, and more than half of the chirp is reduced. Figure 6 presents the impact of frequency detuning under an injection ratio of 5.0. It shows that frequency detuning in either direction increases the CPR value. In contrast to the interband laser, the CPR can be even larger than the free-running laser case for detunings near the stable-locked regime edges. The minimum CPR is obtained at detuning $\Delta\omega_{inj} \approx 0$ GHz (accurately, slightly positive detuning), where the adiabatic chirp is offset by the optical injection dynamics. Through the relationship $\phi = -\tan^{-1} \alpha_H$, the minimum CPR value is given by:

$$CPR_{\min} = \left| j\omega \frac{\phi_1(\omega)}{s_1(\omega)} \right| = \frac{\alpha_H}{2S} \left| \frac{\omega^2}{j\omega + k_c \sqrt{S_{inj}} / S \sqrt{1 + \alpha_H^2}} \right| \quad (12)$$

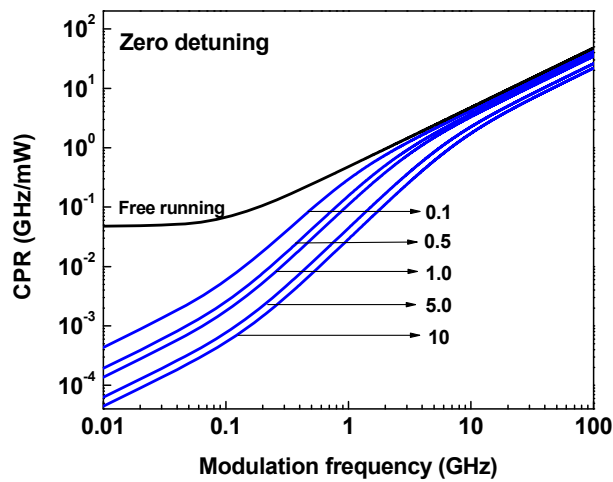


Figure 5. The CPR level for the free-running QC laser and the laser with optical injection at zero detuning. The injection ratio increases from 0.1 up to 10.

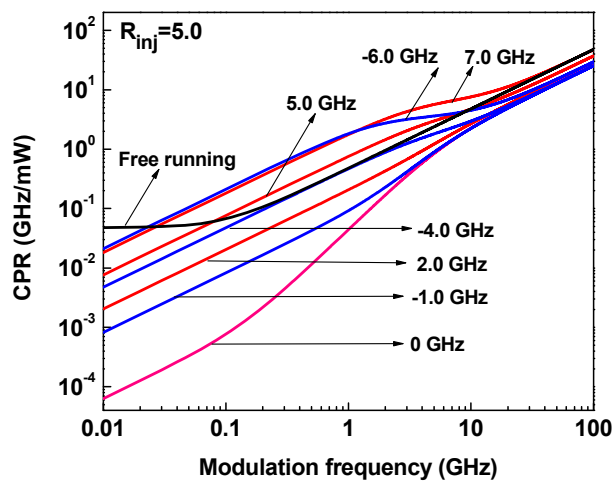


Figure 6. Impacts of frequency detuning to the CPR of the injection-locked QC laser with an injection ratio of 5.0.

The linewidth enhancement factor (LEF) is known to play a crucial role in the characteristics of spectral linewidth broadening, frequency chirp, optical injection as well as optical feedback. The LEF describes the coupling of the carrier-induced variation of the real (refractive index, frequency shift) and imaginary (gain) parts of the susceptibility [25]. Due to the nature of intersubband transitions, QC lasers are expected to exhibit a narrow and symmetric gain spectrum, leading to a zero LEF at the gain peak according to the Kramers-Kronig relation [2]. However, many body Coulomb interactions, coherence of resonant-tunneling transport and electronic dispersion non-parabolicity yields to a non-zero LEF in real QC laser devices. Experimentally reported LEF values range from -2.0 up to 3.0 [26], [27], nevertheless, the LEF of QC lasers in most case is much smaller than that of interband semiconductor lasers. Figure 7(a) shows the impact of the LEF on the modulation response of the injection-locked laser (zero detuning, $R_{inj}=1.0$). Large LEF induces a high peak in the modulation response; however, the modulation bandwidth is hardly influenced. For the frequency chirp in figure 7(b), large LEF increases the CPR of both the free running and the injection-locked lasers. At the modulation frequency of 0.1 GHz, the CPR value is about 10 times enhanced when the LEF increases from 0.1 to 2.0.

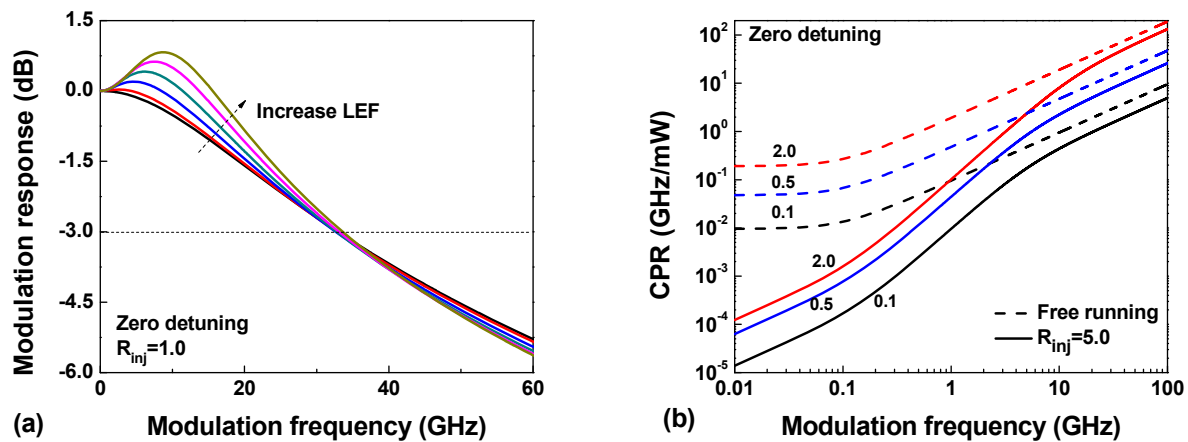


Figure 7. (a) Modulation response at zero detuning with $R_{inj}=1.0$ for various LEF values LEF=0.1, 0.5, 1.0, 1.5, 2.0, 2.5; (b) Impacts of the LEF to the CPR for both the free-running laser and the injection locked laser with $R_{inj}=5.0$.

4. CONCLUSION

The frequency chirp characteristics of an optically injection-locked quantum cascade (QC) laser are theoretically investigated in this work. Based on a macroscopic rate equation model, the key parameter chirp-to-power ratio is analytically derived from the analysis of the differential rate equations. It is found that the CPR of QC lasers can be efficiently reduced by increasing the injection strength, especially at modulation frequencies less than 10 GHz. The frequency detuning of the master laser in either direction will increase the CPR. Since the detuning also enhances the modulation bandwidth in the intensity modulation response, a trade-off is required in the optical injection to simultaneously obtain a large modulation bandwidth and low frequency chirp. These results are of prime importance for improving the QC laser's modulation features for future applications like free-space communications.

ACKNOWLEDGMENTS

Dr. Frédéric Grillot's work is supported in part by the European Office of Aerospace Research and Development (EOARD) under grant FA8655-12-1-2093. Cheng Wang's work is supported by China Scholarship Council.

REFERENCES

- [1] Cornet, C., Dore, F., Ballestar, A., Even, J., Bertru, N., Le Corre, A. and Loualiche, S., "InAsSb/InP quantum dots for midwave infrared emitters: a theoretical study," *J. Appl. Phys.*, 98(12), 126105 (2005).
- [2] Faist, J., Capasso, F., Sivco, D. L., Sirtori, C., Hutchinson, A. L., and Cho, A. Y., "Quantum cascade laser," *Science* 264, 553-556 (1994).

- [3] Capasso, F. *et al*, “Quantum cascade lasers: ultrahigh-speed operation, optical wireless communication, narrow linewidth, and far-infrared emission,” *IEEE J. Quantum Electron.* 38(6), 510-532 (2002).
- [4] Sirtori, C., Nagle, J., “Quantum cascade lasers: the quantum technology for semiconductor lasers in the mid-far-infrared,” *C. R. Physique* 4, 639-648 (2003).
- [5] Paiella, R., Capasso, F., Gmachl, C., Bethea, C. G., Sivco, D. L., Baillargeon, J. N., Hutchinson, A. L., and Cho, A. Y., “High-Speed Operation of Gain-Switched Midinfrared Quantum Cascade Lasers,” *Appl. Phys. Lett.* 75(17), 2536-2538 (1999).
- [6] Paiella, R., Capasso, F., Gmachl, C., Hwang, H. Y., Sivco, D. L., Hutchinson, A. L., Cho, A. Y., and Liu, H. C., “Monolithic Active Mode-Locking of Quantum Cascade Lasers,” *Appl. Phys. Lett.* 77(2), 169-171 (2000).
- [7] Naderi, N. A., Pochet, M., Grillot, F., Terry, N. B., Kovanis, V., and Lester, L. F., “Modeling the injection-locked behavior of a quantum dash semiconductor laser,” *IEEE J. Sel. Top. Quantum Electron.* 15(3), 563-571 (2009).
- [8] Yabre, G., “Effect of relatively strong light injection on the chirp-to-power ration and the 3 dB bandwidth of directly modulated semiconductor lasers,” *J. Lightwave Tech.* 14(10), 2367-2373 (1996).
- [9] Simpon, B. T., and Liu, M. J., “Bandwidth enhancement and broadband noise reduction in injection-locked semiconductor lasers,” *IEEE photon. Technol. Lett.* 7(7), 709-711 (1995).
- [10] Meng, J. X., Chau, T., and Wu, C., M., “Improved intrinsic dynamic distortions in directly modulated semiconductor lasers by optical injection locking,” *IEEE Trans. Microw. Theory Tech.* 47(7), 1172-1176 (1999).
- [11] Chan, S. C., Hwang, S. K., Liu, J. M., “Period-one oscillation for photonic microwave transmission using an optically injected semiconductor laser,” *Optics Express* 15(22), 14921-14935 (2007).
- [12] Hwang, S. K., Liu, J. M., and White, J. K., “Characteristics of period-one oscillations in semiconductor lasers subject to optical injection,” *IEEE J. Sel. Top. Quantum Electron.* 10(5), 974-981 (2004).
- [13] Simpson, T. B., Liu, J. M., Gavrielides, A., and Kovanis, V., “Period doubling route to chaos in a semiconductor laser subject to optical injection,” *Appl. Phys. Lett.* 64(26), 3539-3541 (1994).
- [14] Wang, C., Grillot, C., Kovanis, V. I., Bodyfelt, J. D., and Even, J., “Modulation properties of optically injection-locked quantum cascade lasers,” *Optics Lett.* 38(11), 1975-1977 (2013).
- [15] Wang, C., Grillot, C., Kovanis, V. I., and Even, J., “Rate equation analysis of injection-locked quantum cascade lasers,” *J. Appl. Phys.*, 113(6), 063104 (2013).
- [16] R. Lang, “Injection locking properties of a semiconductor laser,” *IEEE J. Quantum Electron.* QE-18, 976-983 (1982).
- [17] Gensty, T., and Elsaber, W., “Semiclassical model for the relative intensity noise of intersubband quantum cascade lasers,” *Optics Communications* 256, 171-183 (2005).
- [18] Lau, E. K., Wong, L. J., and Wu, M. C., “Enhanced modulation characteristics of optically injection-locked lasers: A tutorial,” *IEEE J. Sel. Top. Quantum Electron.* 15(3), 618-633 (2009).
- [19] Faist, J. *et al*, “Terahertz quantum cascade laser,” *Phil. Trans. R. Soc. Lond. A* 362, 215-231 (2004).
- [20] Sirtori, C., “Quantum cascade laser : fundamentals and performances,” in *Les lasers: applications aux technologies de l’information et au traitement des matériaux*. Les Ulis, France : EDP Science (2002).
- [21] Wiczorek, S., Krauskopf, B., Simpson, T. B., and Lenstra, D., “The dynamical complexity of optically injected semiconductor lasers,” *Physics Reports* 416, 1-128 (2005).
- [22] Dhooge, A., Govaerts, W., and Kuznetsov, Y. A., “MATCONT: A MATLAB package for numerical bifurcation analysis of ODEs,” *ACM TOMS* 29 (2), 141-164 (2003).
- [23] Wiczorek, S., Simpson T. B., Krauskopf, B., and Lenstra, D., “Global quantitative predictions of complex laser dynamics,” *Physical Review E* 65, 045207 (2002).
- [24] Murakami, A., Kawashima, K., and Atsuki, K., “Cavity resonance shift and bandwidth enhancement in semiconductor lasers with strong light injection,” *IEEE J. Quantum Electron.* 39(10), 1196-1204 (2003).
- [25] Osinski, M., and Buus, J., “Linewidth broadening factor in semiconductor lasers—An overview,” *IEEE J. Quantum Electron.* QE-23(1), 9-29 (1987).
- [26] Kumazaki, N., Takagi, Y., Ishihara, M., Kasahara, K., Sugiyama, A., Akikusa, N., and Edamura, T., “Detuning characteristics of the linewidth enhancement factor of a midinfrared quantum cascade laser,” *Appl. Phys. Lett.* 92(12), 121104 (2008).
- [27] Liu, T., Lee, K. E., Wang, Q., J., “Importance of the microscopic effects on the linewidth enhancement factor of quantum cascade lasers,” *Optics Express* 21(23), 27804-27815 (2013).